Characterization of flow unsteadiness in a shock wave turbulent boundary layer interaction by means of Dual-PIV

L.J. Souverein[1,2], B.W. van Oudheusden[1], Fulvio Scarano[1]

[1]*Delft University of Technology, Delft, The Netherlands*
[2]*Institut Universitaire des Systèmes Thermiques Industriels, Marseille, France*

Abstract
The unsteady organization and temporal dynamics of the interaction between a planar shock wave impinging on a turbulent boundary layer at a free stream Mach number of $M_\infty=1.69$ is investigated experimentally by means of dual-plane Particle Image Velocimetry (dual-PIV). Two independent PIV systems were combined in 2 component mode to obtain instantaneous velocity fields separated by a prescribed small time delay. This enables to obtain, in addition to mean and statistical flow properties, also instantaneously time resolved data to characterize the temporal dynamics of the flow phenomenon in terms of time scales, temporal correlations and convective velocities.

Introduction

The effect of a planar shock impinging on a turbulent boundary layer establishes one of the classic interaction phenomena in compressible viscous flow analysis. This particular form of interaction has direct technological relevance to the performance of high speed vehicles, affecting notably the efficiency of supersonic intakes. The renewed attention for the feasibility of sustainable supersonic transport has revived the interest in SWBLI in the moderate supersonic regime. The aim of the current investigation is to contribute to the understanding of the mechanism of unsteadiness that may relate shock motion to upstream and downstream effects (Dolling 2001, Dussauge 2006, Ganapathisubramani 2007).

Conventional two-component PIV measurements have been applied to investigate the statistical and instantaneous organisation of such interactions (see e.g. Humble et al 2006). Although these measurements document the overall flow organization, on the mean as well as instantaneously, information is lacking on its temporal development, as characterized by quantities like time scales, characteristic frequencies and the local acceleration. Due to hardware restrictions on illumination and recording equipment (laser and camera's), the acquisition frequency for PIV is limited to *10 Hz* for conventional systems, and still to typically a few *kHz* for currently available high-speed systems. This is by far insufficient to obtain accurate time-correlated data for flows under these high speed conditions. In the present investigation two independent PIV systems were combined where the time delay between the acquisitions from both PIV systems could be set to arbitrarily small values, not limited by the repetition-rate restrictions of the individual systems. In this way time-correlated data can be obtained as well as acceleration data. One advantage of this approach with respect to the current state of the art high-speed PIV systems is the higher laser power and image resolution. Secondly, it allows setting the delay time between the two PIV systems independent of the pulse separation of the individual systems, as well as permitting very small delay times. The smallest time separation employed in the current investigation was $5\mu s$, corresponding to an effective frequency of *200 kHz*.

Experimental Arrangement

The experiments were performed in the TST-27 transonic supersonic wind tunnel of TU Delft, with test section dimensions of *280 mm* (width) × *255 mm* (height). The wind tunnel is operated as a blow-down facility, with a run time of up to *300 s,* where the Mach number is set by means of a continuously variable throat and flexible upper and lower nozzle walls. Flow conditions for the current investigation are a nominal free stream Mach number of $M_\infty=1.69$ ($U_\infty= 448$ *m/s*), a total temperature of $T_0=276$ *K* and a total pressure of $p_0=2.3$ *bar* resulting in a free stream unit Reynolds number of 35×10^6 m^{-1}. The thickness of the boundary layer is approximately $\delta=17$ *mm.* The boundary layer was assessed to be in fully developed turbulent condition with a Reynolds number based on momentum thickness of approximately *50,000*. The incident shock wave for the SWBLI was generated by a full-span wedge imposing a flow deflection of *6.0*° (see Fig.1).

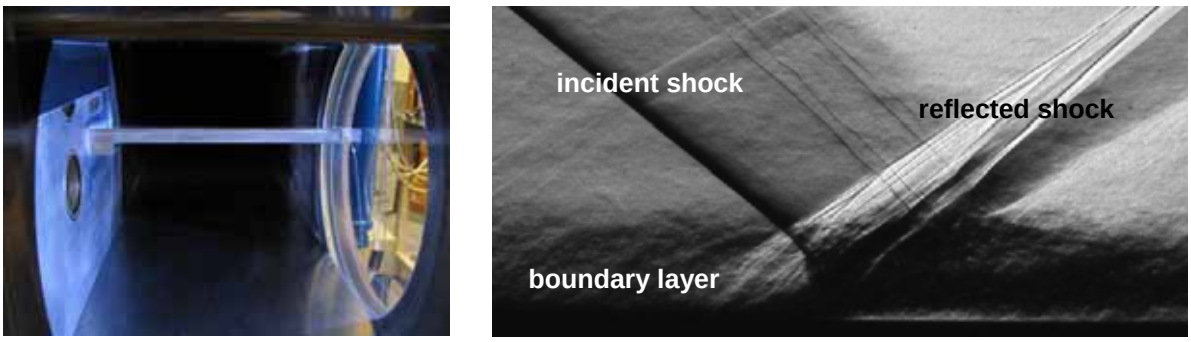

Figure 1: Experimental configuration of the SWBLI experiments; left: the side wall mounted wedge generating the incident shock wave; right: a Schlieren visualisation of a SWBLI.

Dual-PIV setup

The principle op Dual-PIV depends on the mutually independent operation of two two-component (2C) PIV systems. Both systems are aligned to provide illumination in the same measurement plane while observing identical fields of view. The laser light of the two systems was optically separated by means of polarization and the beams of the two lasers were combined and aligned before entering into the light sheet optics. The overlap of the field of view of both cameras was guaranteed by means of a polarizing beam splitter cube, which also assured the independence of the two PIV systems by separating the images based on the polarization. Particular attention was given to the alignment of the FOV of both cameras (Souverein et al. 2007).

The timing-schematic in Fig.2 shows how with a given pulse-delay δt_1, the time separation δt_2 can be set arbitrarily. This allows obtaining time correlated data at different time scales. In the current experiment, the value of δt_2 was varied in the range of *5 μs* to *2000 μs* (corresponding to equivalent frequencies of *200 kHz* to *0.5 kHz*) with an additional reference measurement at *0 μs* delay. The pulse separation δt_1 was kept constant to *1.5 μs* for both laser systems.

The illumination was provided by a Spectra-Physics Quanta Ray laser (*400 mJ/pulse* energy and a *6 ns* pulse duration) and a Quantel laser (*300 mJ/pulse* energy and a *9 ns* pulse duration), installed as lasers 1 and 2 respectively. Both are double-pulsed Nd:Yag lasers with a wavelength of *532 nm*. The light sheet thickness was approximately 2 mm. The flow was seeded with DEHS droplets with an estimated effective particle size of about 1 micron dispersed in the settling chamber of the wind tunnel. The particle images were recorded at 12-bit with a resolution of 1376 × 1040 pixel using a PCO Sensicam QE (camera 1) and a LaVision Imager Intense QE (camera 2). The flow was imaged over a FOV of *76 mm* x *55 mm* (approx. $4\delta \times 3\delta$) at a digital resolution of *55 μm/pixel*. The investigated values of the time separation δt_2 range from 0 to 2000 μs; where per case a dataset of at least 200 image pairs was acquired. The images were interrogated using the WIDIM algorithm (Scarano 1999), employing correlation window deformation with an iterative multi-grid scheme, at 31×31 pixels window size (*1.7 mm* x *1.7 mm*) and an overlap factor of 75%. This resulting measurement grid resolution is 0.43 mm and 0.43 mm in *x* and *y* direction, respectively.

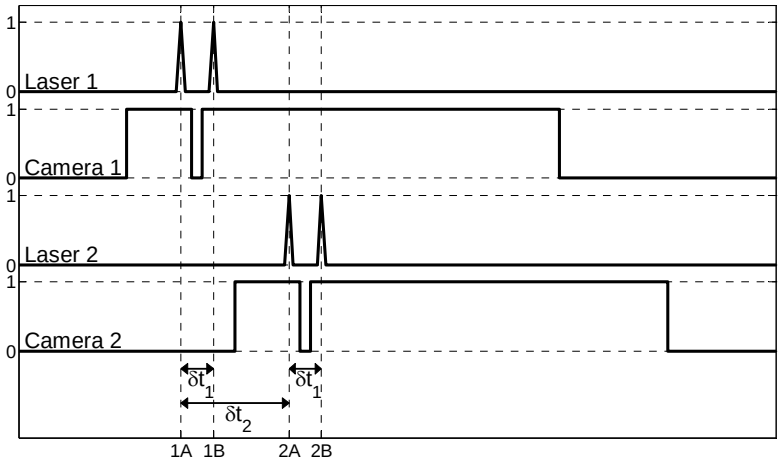

Figure 2: Dual PIV timing diagram.

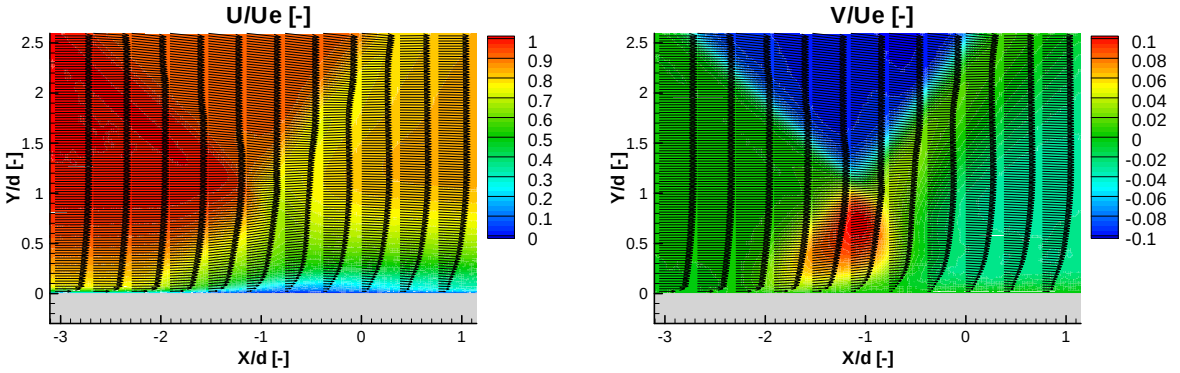

Figure 3: Mean velocity fields; left: u-component, right: v-component

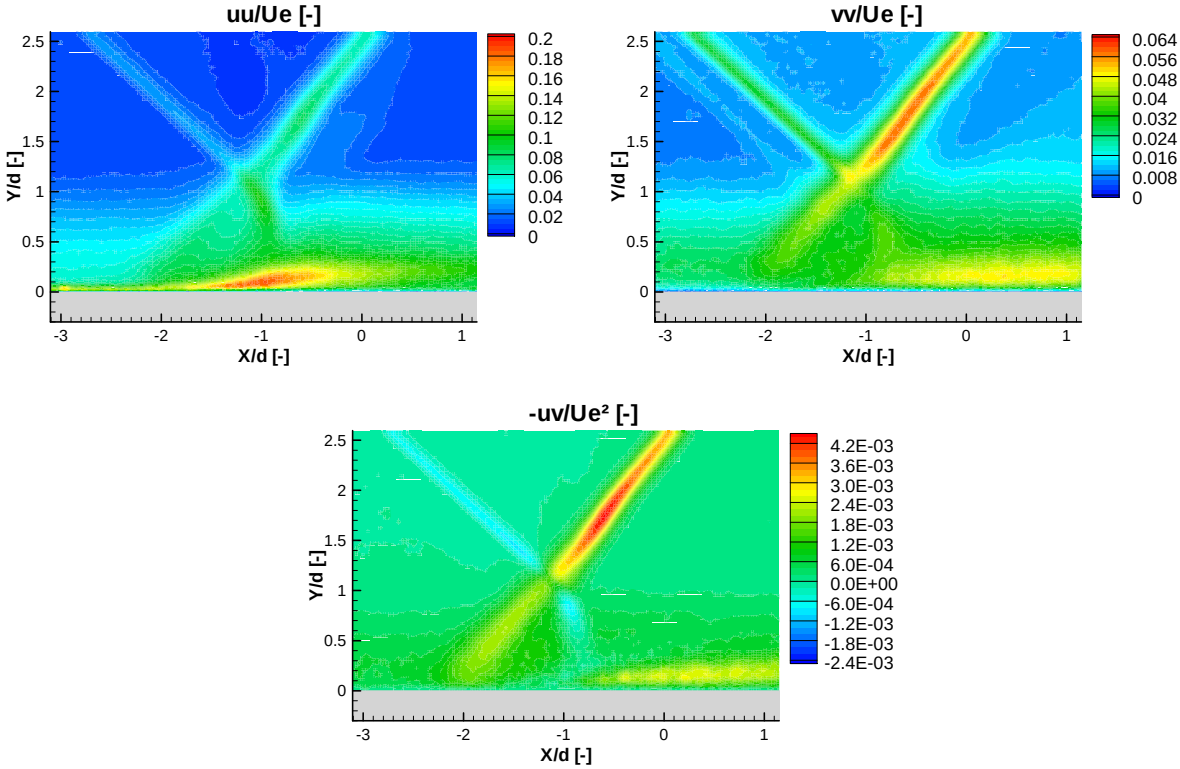

Figure 4: Fluctuation statistics and Reynolds stress; top left: σ_u/U_∞; top right: σ_v/U_∞; bottom: $-\langle u'v'\rangle/U_\infty^2$.

Mean and fluctuation statistics

Figures 3 and 4 show the mean velocity field and the fluctuating velocity statistics respectively, providing a global understanding of the flow topology under consideration. The boundary layer thickness is approximately δ=17mm. The interaction length based on the distance between the extrapolated point of impact of the incident shock and the reflected shock foot is approximately 2δ. The figures show that the incoming boundary layer remains undisturbed within at least the first 10mm (0.5δ) of the FOV. The incident shock wave was observed to be stationary and the local velocity fluctuations observed are attributed to measurement uncertainties. The reflected shock shows strong velocity fluctuations resulting from shock oscillations. The amplitude of the reflected shock excursions based on the vertical velocity component fluctuations is approximately ±5mm. Based on the above observations, the flow under consideration likely presents the case of an incipient separation on the mean.

Determination of time scales

Since measurement were performed for a range of time separations from δt_2=0 µs to 2000 µs, this allows time correlation data for the complete flow field to be obtained as a function of the time delay. This can then be exploited to determine the characteristic time scale at each position in the flow. Specific regions of interest are the incoming boundary layer, the recirculation region where vortex

production and shedding occurs, the reflected shock, and the recovering boundary layer. Figure 5 shows the time correlation coefficient for the u- velocity component, $R_{u_1u_2}$, for different values of the time delay. A first qualitative evaluation of the correlation coefficient shows that for small δt_2 all regions of interest (the incoming boundary layer, the interaction zone and the reflected shock in combination with the expansion fan) remain highly correlated with values close to unity. The incoming boundary layer is the first region to de-correlate, starting from δt_2=*10 μs*, followed by the interaction zone with the initial part of the recovering boundary layer, starting from δt_2=*20 μs*. At *100 μs* all of these regions are de-correlated. The reflected shock with the subsequent expansion still display high correlation values, and also the shear layer, where vortex shedding is initiated, remains slightly correlated. Starting from δt_2=*200 μs* also the reflected shock starts to become de-correlated, still showing medium correlation values up to δt_2=*1000 μs*. The reflected shock no longer appears at δt_2=*2000 μs*, while the expansion fan still displays a weak correlation. This confirms the low frequency behaviour of the reflected shock.

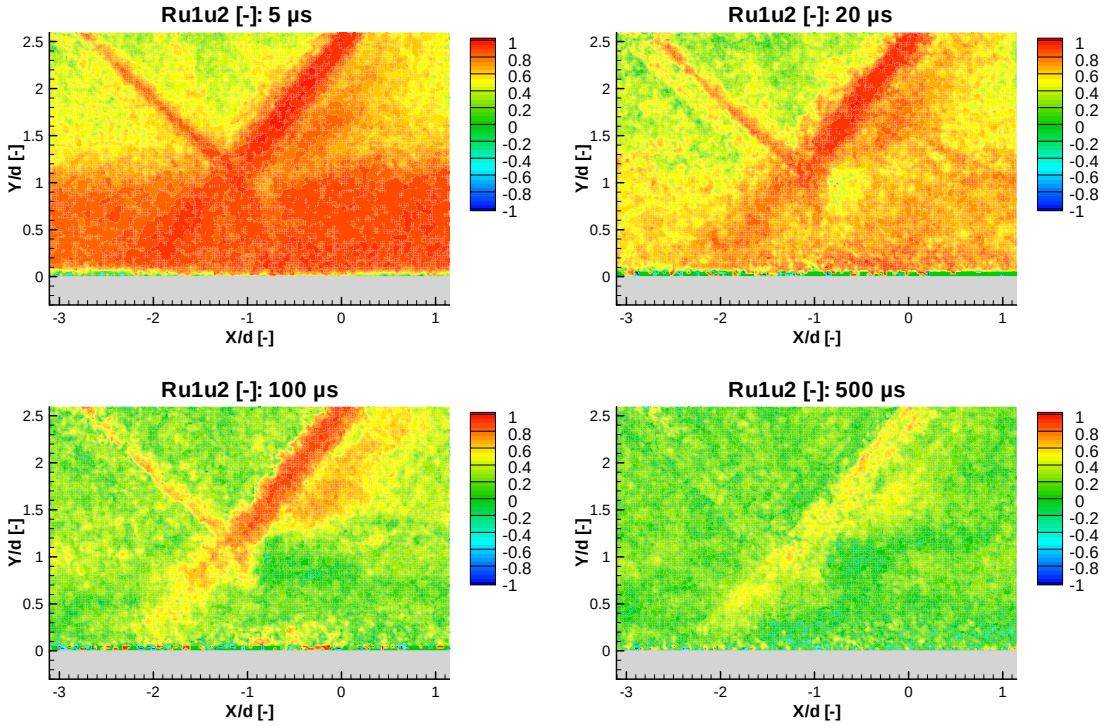

Figure 5: The time correlation coefficient for variable time delay.

References

Dolling DS (2001) Fifty Years of Shock-Wave/Boundary-Layer Interaction Research: What Next? AIAA Journal Vol.39, No.8, August 2001: 1517-1531

Dussauge JP, Dupont P, Debiève JF (2006) Unsteadiness in Shock Wave Turbulent Boundary Layer Interactions with Separations. Aerospace Science and Technology 10: 85-91

Ganapathisubramani G, Clemens NT, Dolling DS (2007) High-speed PIV measurements to study the effect of upstream coherent structures on shock-induced turbulent separation. 7th International Symposium on Particle Image Velocimetry, September 11-14, 2007, Rome, Italy

Humble RA, Scarano F, Van Oudheusden BW (2006) Experimental study of an unsteady impinging shockwave/turbulent boundary layer interaction using PIV, 36th AIAA Fluid Dynamics Conference and Exhibit, 5-8 June 2006, San Francisco, USA, AIAA Paper 2006-3361

Scarano F, Riethmuller ML (1999) Iterative multigrid approach in PIV image processing with discrete window offset. Exp Fluids 26: 513-523

Souverein LJ, Van Oudheusden BW, Scarano F (2007) Determination of time scales in a Shock Wave Turbulent Boundary Layer Interaction by means of Dual PIV, 7th International Symposium on Particle Image Velocimetry, September 11-14, 2007, Rome, Italy